ISSN 2349-0292
Impact Factor 2.365

Global Journal of Advanced Engineering Technologies and Sciences

LOW-TEMPERATURE CO OXIDATION ON Cu/V@h-BN

Nkechi Ibisi[*14], Keke Mao, Wenhua Zhang[2], Xiaojun Wu, Jinlong Yang[1,3]
[*1]Hefei National Laboratory for Physical Sciences at the Microscale, University of Science and Technology of China, Hefei 230026, China.
[2]CAS Key Laboratory of Materials for Energy Conversion.
[3]Department of Chemical Physics, University of Science and Technology of China, Hefei 230026, China.
[4]College of Natural and Applied Sciences, Michael Okpara University of Agriculture Umudike. P. M. B 7267 Umuahia. Abia – State, Nigeria.

Abstract
The catalytic oxidation of CO on Cu-embedded hexagonal boron nitride (h-BN) sheet is investigated using the first-principles method based on density functional theory. Cu atom embeds into the boron monovacancy with high stability and lower formation energy. There is about 0.48e charge transfer from Cu to the hexagonal boron nitride (h-BN) sheet according to the Hirshfeld charge population analysis and the adsorption energy is -5.90eV. The strong adsorption on the surface defect is accompanied by charge transfer to and from the adsorbate. The reaction proceeds via a two-step mechanism of CO + O → OOCO → CO_2 + O and CO + O → CO_2. The energy barriers of the former are 0.47 and 0.26eV respectively, while the latter is a process with energetic drop. The high activity of Cu-embedded hexagonal boron nitride(h-BN) may be attributed to the electronic resonance among electronic states of CO, O_2, and the Cu atom, particularly among Cu-3d, CO-2π*, and O2-2π* orbitals. This good catalytic activity opens a new avenue to fabricate catalyst of low-dimensional material for CO oxidation with lower cost and higher activity.

Keywords: hexagonal boron nitride (h-BN), CO oxidation, DMol3, Cu atom, Density functional theory

Introduction
Catalytic oxidation of CO has been extensively studied because of its importance for CO removal which is a major global environmental concern. This phenomenon has gained prominence for its intrinsic scientific research and immense technological applications.[1,2]

Particularly, these applications include air purification and pollution control devices such as gas mask and car exhaust catalytic converters, hydrogen purification for polymer electrolyte fuel cells and carbon monoxide gas sensors. [3-7] Noble metals such as Pt, Pd, Ru, Rh, and Au are good catalysts for CO oxidation and have been the subject of many studies.[8–14] Recently, due to the increasing price of noble metals and high reaction temperatures special attention has been paid to low cost, high activity and non-noble metal low-temperature CO oxidation.

Many different catalysts have been prepared and tested for low-temperature CO oxidation. [15-19]. The recent progress is rather encouraging low-dimensional materials such as single-layered graphite or graphene. Graphene has been the subject of intensive research [20-24] due to considerable promise for the fabrication of nanoscale devices.[25-27] Moreover the huge surface to volume ratio is advantageous for graphene as a support for heterogeneous catalytic reaction. Hexagonal boron-nitride (*h*-BN) has a similar structure to graphene but in contrast displays unique properties. Indeed *h*-BN is an electrical insulator with a wide band gap (~4.6eV) due to a higher electronegativity of nitrogen and it also exhibits high thermal stability and chemical inertness.[28, 29].

Experimentally, single layer graphene-like *h*-BN nanosheets have been produced on a SiO_2 substrate in the Zettl group.[30] On the theoretical side, Jin et al. and Meyer et al. have respectively fabricated free-standing h-BN single layers by controlled energetic electron beam irradiation through a sputter process.[31,32] These have contributed in opening a new avenue to design advanced catalyst based on *h*-BN.

Atomic defects in *h*-BN have also been characterized and compared to those observed in graphene membranes.[32,33] Azevedo et al. studied defects in *h*-BN monolayer [34,35] however, the formation energy for a single boron (B) vacancy defect (VB) was predicted to be higher than that of a single nitrogen (N) vacancy defect (VN), which contrasts with recent experimental findings.[31,32] Ajun and co-workers performed a density functional theory (DFT) calculation which showed that VB monovacancy has lower formation energy and are more stable in comparison with VN monovacancy in an N-rich environment indicating that the VB defect is preferably formed in an h-BN monolayer. [36] Very recently, Zhao et al reported a theoretical calculation of CO oxidation on Fe-embedded *h*-BN sheet where the Fe atom embeds on the boron monovacancy and the results show that Fe can be constrained at boron vacancy site with a high diffusion barrier (3.70eV) and effectively activate the adsorbed O_2 molecule, thereby exhibiting similar catalytic behavior as compared to the Fe-embedded on the graphene system. [37]

For these reasons, we examined in this paper first principles computation to explore the catalytic performance of non-noble metal Cu-embedded *h*-BN on a single boron vacancy defect for CO oxidation. Our results show that Cu-embedded *h*-BN sheet can serve as a good candidate for efficient catalyst for CO oxidation and it also exhibited similar catalytic behavior as compared to the Cu-embedded graphene system with slightly lower energy barrier.[38] However until now there is no catalytic study of CO oxidation of Cu-embedded on *h*-BN sheet, where Cu atom embeds into the boron monovacancy. Thus pursuing high activity CO oxidation with low dimensional material and further understanding the mechanism is of great interest and importance.

Computation Details

Our spin-unrestricted density functional theory (DFT) calculations were performed with DMOl^3 [40, 41] using generalized gradient approximation (GGA). The exchange – correlation functions were computed within a non local density approximation with Perdew-Burke -Ernzerhof correlation (PBE). [42] DFT semicore pseudopotentials (DSPPs) [43] core treatment was implemented for relativistic effects, which replaced core electrons by a single effective potential. Furthermore, double numerical plus polarization (DNP) was chosen as the basis set and the quality of orbital cutoff is fine.

A *h*-BN supercell (6x6) unit cell containing 72 atoms was treated to a model system where one boron atom was substituted by a Cu atom. A vacuum space of 15Å between two layers was employed which leads to a negligible sheet to sheet interaction. For energy calculations and the transition state search (TS) the brillouin zone integration was performed with 6x6x1 *k*-points sampling since the transverse dimensions of our supercell were large. Optimizations were performed using the gradient convergence method without symmetry constraints. The minimum energy pathway (MEP) for the CO oxidation was calculated using linear synchronous transit (LST/QST) and nudged elastic band (NEB) tools in DMOl^3 code [44] which have been well validated to find TS and MEP. For density of states DOS calculation, the Monkhorst-Pack 6x6x1 *k*-points sampling was used. The cut off global, convergence in energy and force were set to 6.000 angstrom, 10^{-6}eV and 0.050eV respectively. Charge transfers were calculated with the Hirshfeld charge analysis method. [45, 46].

Results And Discussion

Cu-Embedded on hexagonal boron nitride (*h*-BN) with Boron and Nitrogen defects.

We started our study by investigating the adsorption of one Cu atom on hexagonal boron nitride with N and B vacancy defects (V_N and V_B). Here we defined adsorption as $\boldsymbol{E_{ads} = E_{Cu\text{-}vb} - (E_{Cu} + E_{Vb})}$ where $\boldsymbol{E_{Cu\text{-}vb}}$, $\boldsymbol{E_{Cu}}$ and $\boldsymbol{E_{Vb}}$ are the total energies of one Cu atom embedded in *h*-BN with B vacancy, free Cu atom and *h*-BN with B vacancy. Fig 1 shows the geometric and electronic properties of Cu embedded in *h*-BN with N and B vacancy defects. The Cu atom is located on top of the single vacancy defect on both structures forming three bonds with nitrogen in the case of the Boron vacancy while in the Nitrogen vacancy the Cu atom forms three bonds with Boron.

On V_B@*h*-BN, Cu locates at the top of the missed boron atom with an adsorption energy of -5.90 eV and the bond length $d_{(Cu\text{-}N)}$ is 1.83 Å. While the interaction of Cu atom with V_N@*h*-BN is much weaker than V_B@*h*-BN, the adsorption energy is decreased to -2.66 eV and the distance between Cu and neighboring boron atom is elongated to about 2.14 Å. The strong adsorption on the surface defect is accompanied by charge transfer to and from the adsorbate. According to Hirshfeld charge population analysis, on both cases, Cu atom is positively charged with about 0.48 e or 0.15 e transferred from Cu to the V_B@*h*-BN or V_N@*h*-BN sheet. Thus, Cu is trapped more

effectively by the vacancy defect on V_B compared to V_N. This result is in agreement with a theoretical work that has shown that boron monovacancies on *h*-BN are more stable and also easily created than the nitrogen counterpart.[36] This is further supported by a first principle density functional investigation on CO oxidation on Fe-embedded in hexagonal boron nitride.[37] It is noticed that the interaction of Cu with VN@*h*-BN is quite similar with that Au with VN@*h*-BN, thus, it is expected that Cu/V_N@*h*-BN is not an stable catalyst for CO oxidation. On the basis of these we performed our calculations on CO oxidation of Cu-embedded *h*-BN sheet, where the Cu atom embeds into the boron monovacancy.

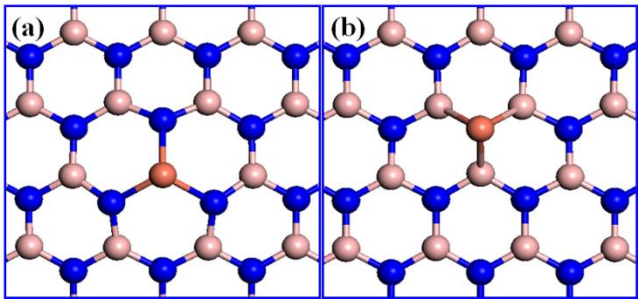

Figure 1. Typical atomic configurations for Cu adsorption on (a) the boron vacancy site of h-BN sheet (b) the nitrogen vacancy site of h-BN sheet. The blue, pink and red ball represents nitrogen, boron and copper atoms respectively.

Adsorption of CO and O_2 on Cu-Embedded *h*-BN sheet

Firstly, the interactions of CO and O_2 with Cu/V_B@*h*-BN sheet are investigated. For O_2 adsorption on Cu/VB@*h*-BN, several adsorption configurations are investigated such as end-on configuration and the parallel configuration. It is suggested the most energetically favorable configuration is characterized by O_2 parallel to the *h*-BN surface forming two chemical bonds with Cu atoms (side-on), and the adsorption energy is -0.55eV which is 0.21eV more favorable than the end-on configuration. There is about 0.48 e charge transfer from the Cu/V_B@*h*-BN sheet to the antibonding $2\pi^*$ orbitals of O_2, which subsequently leads to the elongation of the O-O bond from 1.21 to1.33Å, a typical value for the peroxo species [38]. In comparison to Fe embedded on h-BN the O_2 lies parallel to the *h*-BN surface (end-on configuration) forming one chemical bond with Fe atom.

As for the adsorption of CO on Cu/V_B@*h*-BN, it is found at most stable adsorption configuration CO is tilted with respect to the *h*-BN surface as shown in Fig 2a. The C-O bond length is nearly unchanged as the isolated CO molecule C-O bond length extends from 1.13Å to 1.15Å and the computed adsorption energy is -0.64 eV which is 0.09eV more favorable than the case of O_2 adsorption. Meanwhile, there is 0.06e charge transfer from Cu/*h*-BN to CO which occupies CO-$2\pi^*$ orbital that gave rise or subsequently lead to the increase in C-O bond length. This two structures show similar configurations of CO and O_2 on Cu/graphene system.[39] And it is noteworthy to mention that the bond distance $d_{(Cu\text{-}N)}$ of 1.84Å on Cu/V_B@*h*-BN system and charge transfer of 0.48e from Cu to the *h*-BN sheet compares favorably with bond distance $d_{(Cu\text{-}C)}$ of 1.83Å and charge transfer of 0.37e on the Cu/graphene sheet. Also there is about 0.02e charge transfer from Cu/graphene to CO and subsequent elongation of $d_{C\text{-}O}$ from 1.13 to 1.15Å which is same distance in the $d_{C\text{-}O}$ Cu/h-BN system but the charge transfer is 0.06e. While for O_2, the elongation is 1.21 to 1.35Å on Cu/graphene and 1.21 to 1.33Å in Cu/V_B@*h*-BN for the different charge accumulated on Cu atom. As discussed above, CO and O_2 have comparable adsorption energy on Cu/V_B@*h*-BN and thus, the first adsorption of CO and O_2 should both be considered.

ISSN 2349-0292
Impact Factor 2.365

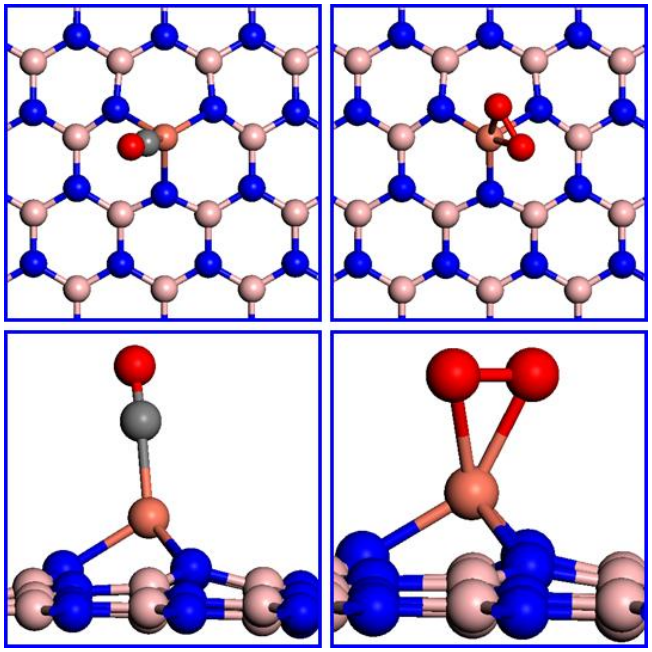

Figure 2. Top and side of views of the geometric structures of CO and O_2 adsorbed on Cu/h-BN respectively.

Mechanisms for the Reaction between the adsorbed O_2 and CO

There are two main established mechanisms for the reaction of O_2 with CO, mainly the Langmuir-Hinshelwood (LH) and the Eley-Rideal (ER) mechanism. The LH involves the coadsorption of O_2 and CO molecules, the formation of an intermediate state and desorption of CO_2 molecule. In ER mechanism, gas phase CO (O_2) molecule approaches the pre-adsorbed O_2 (CO) molecule. We have studied the adsorption of CO (O_2), the coadsorption behavior of CO and O_2 as well as the effect of preadsorption of O_2 on the sequential adsorption of the CO molecule on the Cu/V_B@h-BN system. Generally, the gas molecule adsorption ability determines the reaction pathways on the catalyst therefore we have investigated both the Eley-Rideal (ER) and Langmuir Hinshelwood (LH) mechanisms of CO oxidation in our study.

The small adsorption energy difference of O_2 and CO molecules (0.55 and 0.64 eV) on Cu/*h*- BN system indicates that there is a certain probability of having either O_2 or CO adsorbed on Cu. Additionally, the slightly larger adsorption energy of CO compared with the O_2, could cause the active site of Cu to be covered by CO if CO/O_2 is injected as the reaction gas. In this case the Cu active site would be blocked which hinders the ER reaction. Instead the coadsorption of the CO and O_2 on the Cu/*h*-BN system and the LH reaction should be favored. Hence, two mechanisms (the ER and LH) were studied to clarify the favorable catalytic oxidation pathway of CO on the Cu/h-BN system.

To search for the minimum-energy pathway (MEP) for CO oxidation, several coadsorption configurations via the LH mechanism were tested. We selected the most stable co-adsorption configuration as an initial state (IS), CO is in the gas phase and O_2 is slightly tilted to the *h*-BN sheet. We find that the dissociative adsorption of O_2 on Cu atom is energetically unfavorable when O_2 interacts with Cu/V_B@*h*-BN system, thus the ER mechanism is hardly possible in our case as a starting point. This is similar to the case of CO oxidation on Cu-embedded in a graphene system.[39] Therefore the LH reaction of CO + O → OOCO → CO_2 + O was the starting point and the ER reaction of CO + O → CO_2 followed as a two-step process.

We examined two pathways for LH and part 2 (fig 5) is more favorable than part 1 (fig 4). Where the CO and O_2 coadsorbed while tilting towards the h-BN sheet.

ISSN 2349-0292
Impact Factor 2.365

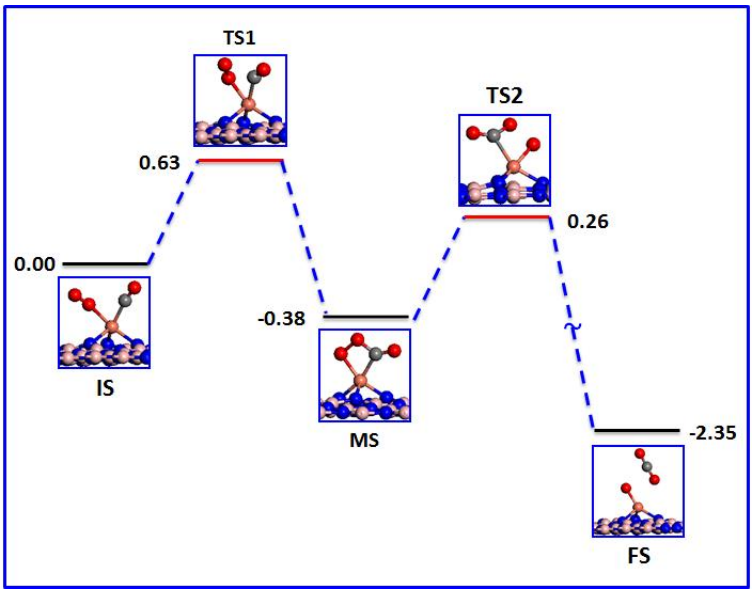

Figure 4. Potential energy profile along the minimum-energy pathway for CO oxidation via CO + O_2 → OOCO → CO_2 + O route. All energies are given with respect to the reference energy, ie the sum of the Cu-embedded h-BN sheet and individual O_2 and CO molecules. The local configurations of the adsorbates on the Cu/h-BN sheet at initial state (IS), transition state (TS), and final state (FS) along the minimum-energy pathway are shown in the inserts respectively.

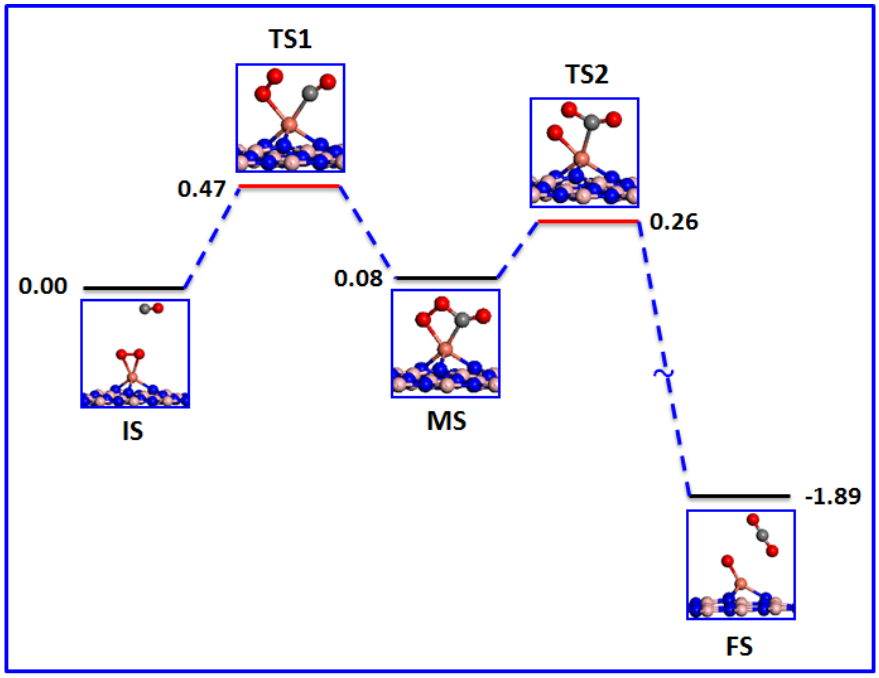

Figure 5. Potential energy profile along the minimum-energy pathway for CO oxidation via CO + O_2 → OOCO → CO_2 + O route. All energies are given with respect to the reference energy, ie the sum of the Cu-embedded h-BN sheet and individual O_2 and CO molecules. The local configurations of the adsorbates on the Cu/h-BN sheet at initial state (IS), transition state (TS), and final state (FS) along the minimum-energy pathway are shown in the inserts respectively.

ISSN 2349-0292
Impact Factor 2.365

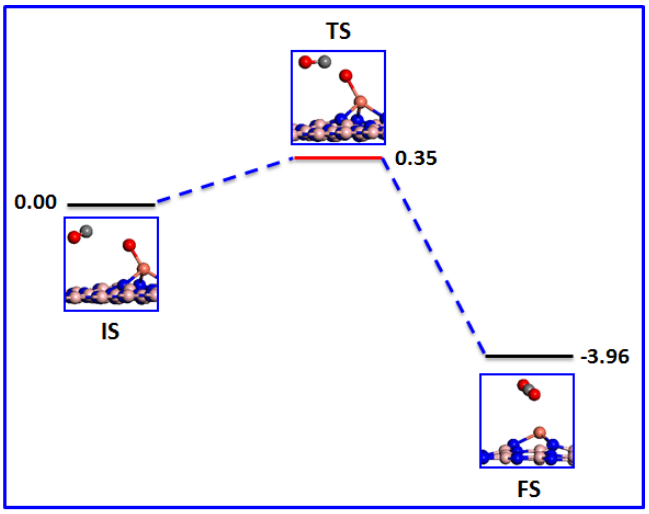

Figure 6. Potential energy profile along the minimum–energy pathway for CO oxidation via the CO + O → CO_2 route. (ER) All energies are given with respect to the reference energy, ie the sum of the Cu-embedded h-BN sheet and individual O atom and CO molecule. The local configurations of the adsorbates on the Cu/h-BN sheet at initial state (IS), transition state (TS), and final state (FS) along the minimum-energy pathway are shown in the inserts respectively.

Once CO and O_2 are co adsorbed on Cu/BN system, one of the oxygen atoms O_2 approaches C of CO and reaches TS1. The energy barrier (E_r) along MEP is estimated to be 0.47eV. Meanwhile a peroxo-type O1-O2-C-O complex is formed above Cu atom. Passing over TS1, the complex is still maintained until a metastable configuration (MS) is reached. The bond length *d*(O-O) of oxygen increases from 1.33 – 1.50Å in this reaction. The reaction proceeds continuously from MS to FS with a relatively lower energy barrier of 0.26eV (TS2), where CO_2 is formed through an exothermic reaction, leaving an atomic oxygen O adsorbed on the Cu/*h*-BN sheet.

The overall barrier in a catalytic system is of importance than a particular barrier. Therefore for this system, though the first reaction was endothermic (0.08eV) the energy value is relatively low and as such the overall barrier is 0.47eV. We also checked whether CO oxidation with atomic oxygen O is conceivable after CO_2 is formed (ER mechanism). It was found that the reaction can proceed with an energy barrier of 0.35eV and the reaction is also exothermic.

Conclusion

In summary, we have investigated theoretically the reaction of carbon monoxide with oxygen on Cu/*h*-BN system, aiming to explore the catalytic activity of Cu/*h*-BN system with Cu embedded on a boron vacancy site. The reaction proceeds via LH reaction as the first reaction step with activation barrier of 0.47eV, followed by ER reaction with a smaller energy barrier of 0.35eV. Both reactions are exothermic. The second pathway with a higher barrier of 0.64eV is also feasible since it is lower than the value for most noble-metal catalyst which is usually within the range of 1eV and above. The catalytic activity of Cu-embedded on *h*-BN can be attributed to the partially occupied Cu-3d orbital being crucial for the activity and it is localized around the vicinity of the Fermi level (E_F) due to interaction between Cu atom and h-BN. Also the electronic resonance among the CO-2π* and O2-2π* orbitals are strong contributory factors to the catalytic activity as well. Hence the Cu/*h*-BN is a good candidate for CO oxidation with lower cost and higher activity.

ACKNOWLEDGMENTS

This work was financially supported by National Natural Science Foundation of China (21103156,), National Basic Research Program of China (2013CB933104, 2010CB923301), MOE Fundamental Research Funds for the Central Universities. by the USTC-HP HPC project, by the USTC-Lenovo 1800 project and Shanghai Supercomputer Center.

References

1. G. Ertl, Chem. Record, 1, (2001) 33
2. T. Engel and G. Ertl, in The Chemical Physics of Solid Surfaces and Heterogeneous Catalysis, edited by D. A. King and D. P. Woodruff (Elsevier, New York, 1982), Vol. 4;
3. X. Yu, S. Ye, J. Power Sour. 172 (2007) 145.
4. J. T. Kummer, *J. Phys. Chem*. *90*, (1986), 4747.
5. M. V. Twigg, Appl. Catal. B 70, (2007) 2–15
6. D.R. Schryer, B.T. Upchurch, B.D. Sidney, K.G. Bromn, G.B. Hoflund, P.K. Herz, J. Catal. 130 (1991) 314
7. H. Okamoto, H. Obayashi, and T. Kudo, Solid State Ionics, 1, 3, (1980) 319
8. G. Ertl, Angew. Chem. 120, (2008) 3578; Angew. Chem. Int. Ed. 47, (2008) 3524.
9. S. M. McClure, M. J. Lundwall, D.W. Goodman, Proc. Natl. Acad. Sci. USA 106, (2009) 1–6.
10. A. Binder,M. Seipenbusch, M. Muhler,G. Kasper, J. Catal. 268, (2009) 150 – 155.
11. I. E. Beck, V. I. Bukhtiyarov, I. Y. Pakhurakov, V. I. Zaikovsky, V. V. Kriventsov, V. N. Parmon, J. Catal. 268, (2009) 60 – 67.
12. M. Haruta, Nature 437, (2005) 1098 – 1099
13. M. Okumura, N. Masuyama, E. Konishi, S. Ichikawa, T. Akita, J. Catal. 208 (2002) 485.
14. G. Avgouropoulos, T. Ioannides, Ch. Papadopoulou, J. Batista, S. Hocevar, H.K. Matralis, Catal. Today 75 (2002) 157
15. D.R. Schryer, B.T. Upchurch, J.O. van Norman, K.G. Brown and J. Schryer, J. Catal. 122 (1990) 193.
16. D.S. Stark and M.R. Harris, J. Phys. E 21 (1988) 715
17. M. Haruta, S. Tsubota, T. Kobayashi, A. Ueda, H. Sakurai and M. Ando, Stud. Surf. Sci. Catal. 75 (1993) 2657.
18. S. Tsubota, A. Ueda, H. Sakurai, T. Kobayashi and M. Haruta, Am.Chem. Soc. Symp. Ser. 552 (1994) 420.
19. X. Xie, Y. Li, Z. Liu, M. Haruta, W. Shen, Nature 458, (2009), 746
20. A. K. Geim, K. S. Novoselov, *Nat. Mater. 6*, *(*2007) 183
21. S. Gilje, S. Han, M. Wang, K. L. Wang and R. B. Kaner, *Nano Lett.*, 7, (2007), 339
22. D. W. Boukhvalov, M. I. J. Katsnelson, Phys. Chem. C 113, (2009), 14176
23. P. Blake, P. D. Brimicombe, R. R., Nair, T. J. Booth, D. Jiang, F. Schedin, L. A., Ponomarenko, S. V. Morozov, H. F. Gleeson, E. W. Hill, A. K. Geim, and K. S., Novoselov, *Nano Lett.*, 8, (2008),1704
24. T. J. Booth, P. Blake, R. R, Nair, D. Jiang, E. W. Hill, U. Bangert, A. Bleloch, M. Gass K. S. Novoselov, M. I Katsnelson, and A. K Geim, *Nano Lett.*, 8, (2008), 2442
25. V. Falko, *Nat. Phys. 3*, *(*2007), 151.
26. A. Du, Z. Zhu, and S. C. Smith, *J. Am. Chem. Soc.*, 132, 9, (2010), 2876
27. A. Du, S. Sanvito, Z. Li, D. Wang, Y. Jiao, T. Liao, Q. Sun, Y. H. Ng, Z. Zhu, R. Amal, and S.C. Smith, *J. Am. Chem. Soc.*, 134, 9, (2012), 4393
28. C. H. Park, S. G. Louie, Nano lett. 8 (2008) 2200.
29. K. S. Novoselov, D. Jiang, F. Schedin, T. Booth, V. V. Khot-kevich, S. Morozov, A. K. Geim, *Proc. Natl. Acad. Sci. U.S.A.* 102, (2005), 10451.
30. D. Pacile, J. C. Meyer, C. O. Girit, A. Zettl, Appl. Phys. Lett. 92, (2008), 133107.
31. C. H. Jin, F. Lin, K. Suenaga, S. Iijima, Phys. ReV. Lett. 102, (2009), 195505.
32. J. C. Meyer, A. Chuvilin, G. Algara-Siller, J. Biskupek, U. Kaiser, Nano Lett. 9, (2009), 2683.
33. A. Zobelli, C. P. Ewels, A. Gloter, G. Seifert, *Phys. Re*V. *B 75*, *(*2007), 094104.
34. S. Azevedo, J. R. Kaschny, C. M. C. de Castilho, F. de Brito Mota, Nanotechnology 18, (2007), 495707.
35. S. Azevedo, J. R. Kaschny, C. M. C. de Castilho, F. de Brito Mota, Eur. Phys. J. B 67 (2009), 507.
36. A. Du, Y. Chen, Z. Zhu, R. Amal, G.Q. Lu, S.C. Smith, J. Am. Chem. Soc. 131 (2009) 17354.
37. P. Zhao, Y. Su, Y. Zhang, S. J. Li, G. Chen, Chemical Physics letters 515, (2011) 159
38. G.L. Gutsev, B.K. Rao, P. Jena, J. Phys. Chem. A 104 (2000) 11961
39. E. H. Song, Z. Wen, Q. Jiang, J. Phys. Chem. C 115, (2011) 3678
40. B. J. Delley, Chem. Phys. 92, (1990), 508.
41. B. J. Delley, Chem. Phy. 113, (2000), 7756.
42. J. P. Perdew, k. Burke, M. Ernzerhof, Phys. Rev. let. 77, (1996) 3865
43. B. Phys. Delley, Rev. B 66, (2002), 155125.
44. G. Henkelman, H. Jonsson, *J. Chem. Phys.*, **113,** (2000) 9978

45. F. L. Hirshfeld, *Theor. Chim. Acta B*, **44**, (1977) 129
46. Delley, B. *Chem. Phys.*, **110,** (1986) 329